Linear Rod−Coil Multiblock Oligomers with a Repeating Unit-Dependent Supramolecular Organization

Myongsoo Lee* and Byoung-Ki Cho

Department of Chemistry, Yonsei University, Shinchon 134, Seoul 120-749, Korea

Nam-Keun Oh and Wang-Cheol Zin

Department of Materials Science and Engineering, Pohang University of Science and Technology, Pohang 790-784, Korea

Received November 13, 2000; Revised Manuscript Received January 8, 2001

ABSTRACT: A series of linear rod−coil multiblock oligomers of the $(rod-coil)_n$ type (n = 1, 2, 3, 13) consisting of a rigid rod segment made up of three biphenyls connected though methylene ether linkages and a poly(propylene oxide) with degree of polymerization of 13 as a coil segment were prepared, and their thermal behavior and supramolecular organization in the solid and melt states were investigated. In opposition to the behavior of conventional oligomers, transition temperatures of these multiblock oligomers associated with both crystalline melting and isotropization decrease with increasing the number of repeating units (n). Small- and wide-angle X-ray diffraction investigations were carried out to elucidate the details of supramolecular structure. All of the oligomers were observed to be self-organized into ordered supramolecular structures that differ significantly on variation of the number of repeating units. The $(rod-coil)_1$ shows a lamellar crystalline and a bicontinuous cubic liquid crystalline structures. In contrast, the $(rod-coil)_2$ shows a 2-D rectangular crystalline and a tetragonal columnar liquid crystalline structures, while the $(rod-coil)_3$ and the $(rod-coil)_{13}$ display a hexagonal columnar structure in both their solid and melt states. These results demonstrate that systematic variation of the number of repeating units in the rod−coil multiblock oligomers can provide a strategy to regulate the supramolecular structure, from 1-dimensional lamellar, 2-dimensional rectangular to 2-dimensional hexagonal structures in the solid state and from bicontinuous cubic, tetragonal columnar to hexagonal columnar in the melt state.

Introduction

Spontaneous organization phenomena in synthetic molecules and macromolecules offer a means to construct a variety of ordered nanostructures with well-defined shape and size which have potential fundamental and practical implications in areas such as materials science, molecular electronics, and biomimetic chemistry.[1−5] A typical example is provided by block copolymers, where the repulsion between the covalently connected segments leads to self-organization into lamellar, cylindrical, spherical, and other structures.[4,6] Even more complicated structures have been created with the presence of stiff rodlike segment to which a flexible coil segment is covalently attached.[1,7,8] This rod−coil molecular architecture imparts microphase separation of the rod and coil blocks into ordered periodic structures in nanoscale dimensions due to the mutual repulsion of the dissimilar blocks and the packing constraints imposed by the connectivity of each block, while the anisometric molecular shape and stiff rodlike conformation of the rod segment imparts orientational organization. To balance these competing parameters, rod−coil molecules self-organize into a variety of supramolecular structures which can be controlled by variation of the rod-to-coil volume fraction.

Recent observations from our laboratory have shown that the rod−coil diblock molecules containing poly(propylene oxide) as a coil segment self-assemble into layered smectic, bicontinuous cubic, and hexagonal columnar liquid crystalline superlattices as a function of coil volume fraction.[9] In a preliminary communication,[10] we have demonstrated that introduction of a hydrophobic docosyl chain into the rod−coil diblock molecule containing hydrophilic poly(ethylene oxide) coil gives rise to the formation of a discrete micellar phase with a lack of 3-D symmetry. In contrast, the coil−rod−coil ABA triblock molecules based on poly(propylene oxide) as a coil segment have proven to be self-assemble into discrete rod bundles which organize into a 3-D tetragonal structure.[11] In addition, we have shown that the rod−coil approach as a means to manipulate supramolecular structure could be extended to main chain rod−coil multiblock copolymer systems which generate bicontinuous cubic and hexagonal columnar phases depending on the rod-to-coil volume fraction.[12] Our results on rod−coil systems suggest that one of the important parameters for creation of novel supramolecular structure is the relative coil volume fraction to rod.

A novel strategy to manipulate the supramolecular structure at constant rod-to-coil volume ratio can also be accessible by varying the number of grafting sites per rod which may be closely related to the grafting density at the interface separating rod and coil segments. Systematic variation in the number of grafting sites per rod is expected to be easily achieved by serial combinations of rod−coil constituting units which give rise to rod−coil multiblock oligomers of $(rod-coil)_n$ type (n = 1, 2, 3, 13). A $(rod-coil)_1$ has a rod grafted by a coil at only one end which gives rise to a lower grafting density at the interface. As the number of repeating units (n) increases, the average number of grafting sites per rod increases. Consequently, all rods of a rod−coil

* To whom correspondence should be addressed. Fax 82-2-364-7050; E-mail mslee@yonsei.ac.kr.

10.1021/ma001938f CCC: $20.00
Published on Web 02/13/2001

Table 1. Characterization and Thermal Transitions of (Rod−Coil)$_n$ (Data Are from the Second Heating and the First Cooling Scans)[a]

			phase transitions (°C) and corresponding enthalpy changes (kJ/mru[b])	
n	$\bar{M}_w/\bar{M}_n$ (GPC)	n_{graft}[c]	heating	cooling
1	1.04	1	k_1 154.4 (8.4) k_2 194.2 (1.1) k_3 212.3 (7.4) cub 233.4 (1.6) i	i 222.6 (1.5) cub 202.8 (7.5) k_3 161.8 (0.9) k_2 123.8 (7.9) k_1
2	1.05	1.5	k 168.0 (6.2) col_t 191.0 (1.8) i	i 186.2 (1.8) col_t 161.9 (6.3) k
3	1.08	1.67	k 143.9 (5.1) col_h 183.8 (1.7) i	i 177.9 (1.5) col_h 140.9 (4.5) k
13	1.29	1.92	g −42.5 k 94.0 (3.5) col_h 180.3 (1.4) i	i 170.9 (1.3) col_h 84.3 (3.4) k −44.3 g

[a] g = glassy, k = crystalline, col_t = tetragonal columnar, col_h = hexagonal columnar, i = isotropic. [b] mru = mole repeating unit. [c] n_{graft} = average number of grafting sites per rod.

multiblock copolymer with infinite number of repeating units are grafted by coils at the both ends, where considerable crowding at the interface may occur due to a higher grafting density. To relieve this additional crowding, the domain structure assembled by (rod−coil)$_1$ will be transformed into those with larger interfacial area. This implies that serial combinations of rod−coil constituting units give rise to unique rod−coil multiblock oligomers with a repeating-unit-dependent organization. With this in mind, we have synthesized (rod−coil)$_1$, (rod−coil)$_2$, (rod−coil)$_3$, and (rod−coil)$_{13}$ containing poly(propylene oxide) with degree of polymerization (DP) of 13 as a coil segment and investigated their organization behavior in the crystalline and liquid crystalline states. Since the rod−coil multiblock oligomers are all based on the same constituting unit, the supramolecular structural change can only be attributed to the variation of coil grafting fraction per rod.

We report here on the synthesis of linear rod−coil multiblock oligomers (i.e., (rod−coil)$_1$, (rod−coil)$_2$, and (rod−coil)$_3$) and (rod−coil)$_{13}$ consisting of a rigid rod segment made up of three biphenyls connected through methylene ether linkages and a poly(propylene oxide) (PPO) with DP of 13 as a coil segment and their self-assembling behavior characterized by optical polarized microscopy, differential scanning calorimetry (DSC), and X-ray diffraction measurements. These rod−coil multiblock oligomers self-organize into successively lamellar, 2-D rectangular and 2-D hexagonal columnar structures in the solid state and 3-D bicontinuous cubic, 2-D tetragonal, and 2-D hexagonal columnar structures in the melt state as the number of rod−coil repeating unit increases.

Results and Discussion

Synthesis of Rod−Coil Multiblock Oligomers and Polymer. Scheme 1 outlines the synthesis of linear (rod−coil)$_1$, (rod−coil)$_2$, and (rod−coil)$_3$. The repeating unit of rod−coil oligomers consists of three biphenyl units connected by methylene ether linkages as a rod block and poly(propylene oxide) with DP of 13 as a coil block. To exclude the effect of terminal groups on their phase behavior, all of the oligomers are grafted by methoxy groups at both chain ends. (Rod−coil)$_1$ precursor molecule **3** was synthesized by etherification of **2** with 4,4′-bis(bromomethyl)biphenyl in the presence of potassium carbonate. The subsequent etherification of **3** with 4-hydroxy-4′-methoxybiphenyl produced (rod−coil)$_1$ **4**. (Rod−coil)$_2$ precursor **5** was synthesized by etherification of **3** with biphenol-terminated poly(propylene oxide) and then the subsequent reaction with 4,4′-bis(bromomethyl)biphenyl. Resulting precursor molecule **5** was treated with 4-hydroxy-4′-methoxybiphenyl to yield (rod−coil)$_2$ **6**. (Rod−coil)$_3$ **8** was synthesized by following the same sequence of reactions, i.e., by etherification of **5** with biphenol-terminated poly(propylene oxide) and then the subsequent reaction with 4,4′-bis(bromomethyl)biphenyl and finally reaction with 4-hydroxy-4′-methoxybiphenyl.

All of the resulting linear rod−coil multiblock oligomers were purified by silica gel column chromatography as described in Experimental Section until transition temperatures remained constant. All analytical data of the rod−coil multiblock oligomers were consistent with expected molecular structures. Molecular weight distributions of these oligomers determined from gel permeation chromatography (GPC) with polystyrene standards appeared to be less than 1.08 as shown in Table 1. To compare the phase behavior of the oligomers to that of long chain homologue, the rod−coil multiblock copolymer was synthesized by condensation reaction from biphenol-terminated poly(propylene oxide) with the number of propylene oxide units of 13 and bis(bromomethyl)biphenyl according to the procedure described previously.[12]

The relative molecular weight determined from GPC with polystyrene standards is expected to be much higher than the absolute value since the hydrodynamic volume of the polymer based on rigid rod units is larger than that of the polystyrene standards with similar molecular weights.[13] Therefore, the molecular weight and the molecular weight distribution of the rod−coil multiblock copolymer were determined by using a calibration plot constructed with the rod−coil multiblock oligomers since the theoretical log molecular weights of the rod−coil multiblock oligomers show a linear dependence on elution volume. The degree of polymerization (DP) and molecular weight distribution of the copolymer appeared to be 13 and 1.29, respectively, which are believed to be close to the absolute values. It should be noted that all of the oligomers and polymer represent to have the same coil volume fraction relative to rod since they are based on the same rod−coil constituting unit.

Thermal Characterization. Self-assembled structures of the oligomers and polymer were investigated by means of optical polarized microscopy and differential scanning calorimetry (DSC) in combination with small- and wide-angle X-ray scatterings (SAXS and WAXS). Figure 1 shows the DSC heating and cooling traces of the (rod−coil)$_1$, (rod−coil)$_2$, (rod−coil)$_3$ and the polymer. The transition temperatures together with the corresponding enthalpy changes are summarized in Table 1. (Rod−coil)$_1$ **4** displays crystal-to-crystal transitions at 154 and 194 °C and a melting transition at 212 °C on the DSC heating scan. On further heating, the highest temperature crystalline phase melts into an optically isotropic cubic phase.

Scheme 1. Synthesis of Rod−Coil Multiblock Oligomers

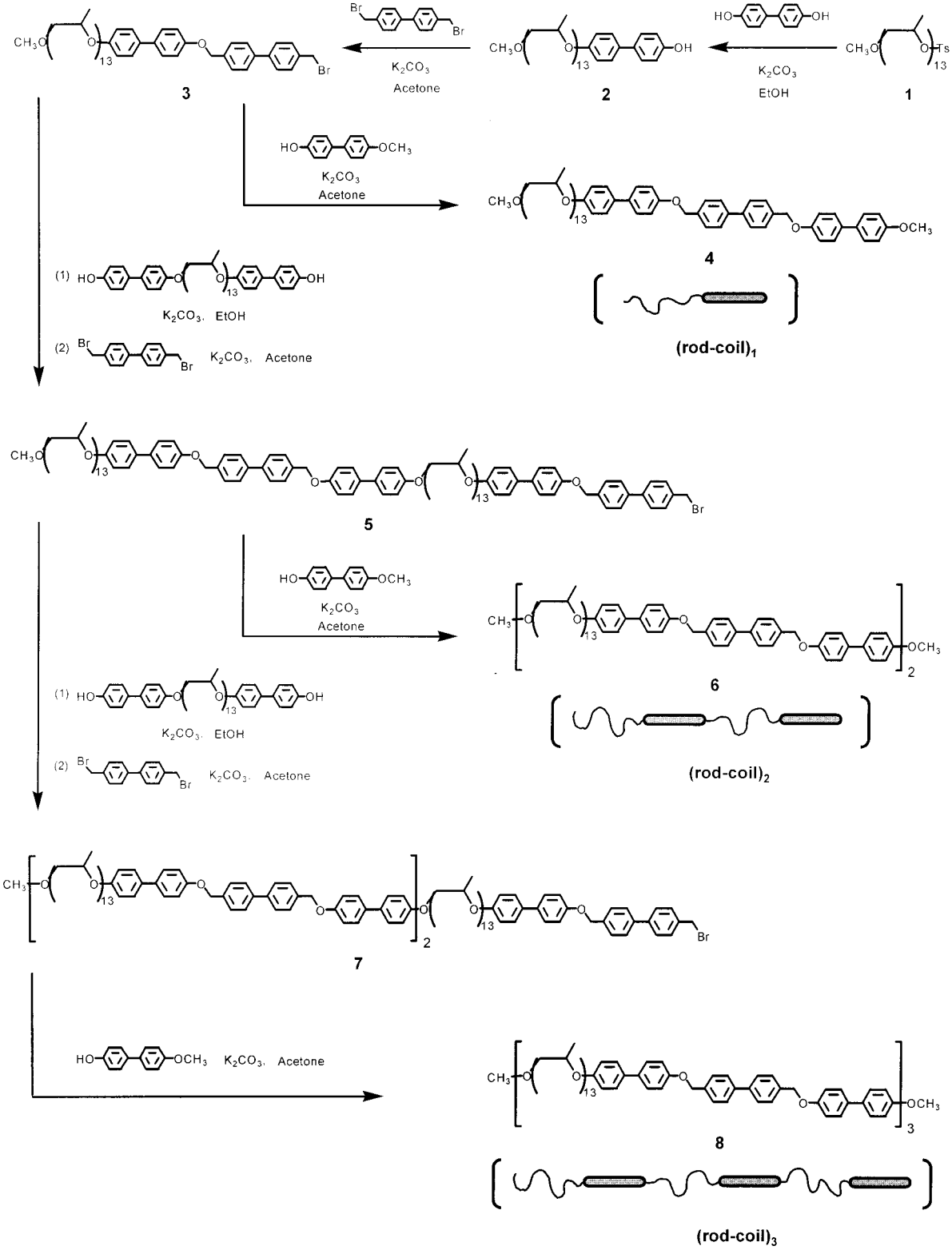

In contrast to the (rod−coil)$_1$, (rod−coil)$_2$ **6** shows a tetragonal columnar liquid crystalline phase. DSC investigations revealed that the (rod−coil)$_2$ exhibits a crystalline melting transition at 168 °C, followed by a liquid crystalline phase which undergoes transformation into an isotropic liquid at 191 °C. On slow cooling from the isotropic liquid, the formation of unique domains growing in four directions which coalesce into a mosaic texture could be easily observed on the polarized optical microscope, indicating the presence of a tetragonal mesophase (Figure 2).[11,14]

(Rod−coil)$_3$ **8** exhibits a birefringent solid, which melts at 143.9 °C into a liquid crystalline phase and then is transformed into an isotropic phase at 183.8 °C. On the polarized optical microscope, a transition from an isotropic liquid can be identified by the formation of a pseudo-focal conic texture which is characteristic of a hexagonal columnar mesophase.[9] The polymer also

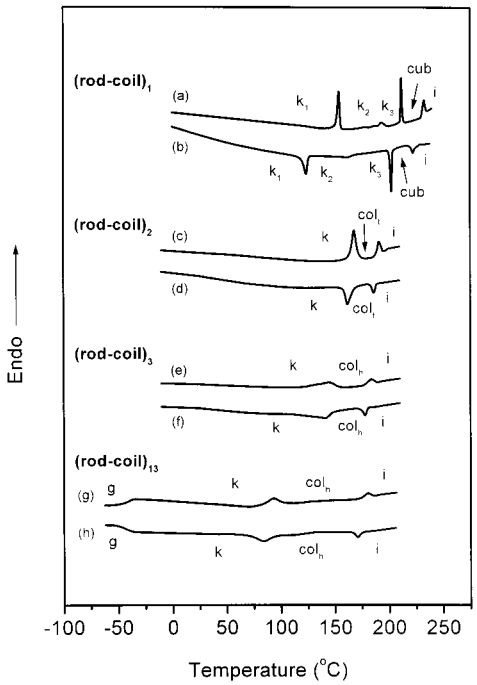

Figure 1. DSC traces (10 °C/min) recorded during the second heating scan (a), the first cooling scan (b) of the $(rod-coil)_1$, the second heating scan (c), the first cooling scan (d) of the $(rod-coil)_2$, the second heating scan (e), the first cooling (f) of the $(rod-coil)_3$, the second heating scan (g), and first cooling scan (h) of the $(rod-coil)_{13}$.

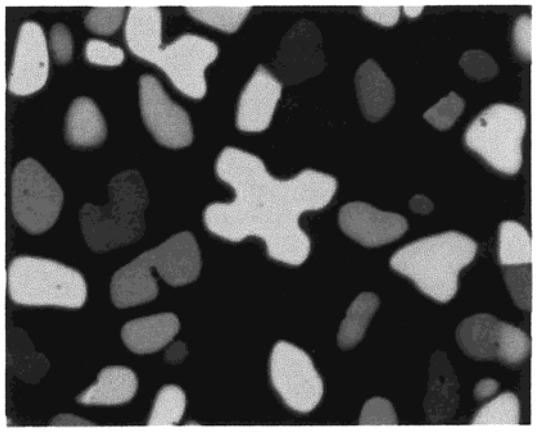

Figure 2. Representative optical polarized micrograph (100×) of the texture exhibited by the tetragonal columnar mesophase of the $(rod-coil)_2$ at the transition from the isotropic liquid at 185 °C.

shows phase behavior similar to that of the $(rod-coil)_3$, which exhibits a crystalline melting, followed by a hexagonal columnar liquid crystalline phase.

The thermal behavior of the oligomers and the polymer determined from the heating DSC scans as well as thermal optical polarized microscopy is presented in Figure 3. In opposition to conventional oligomers based on rigid rod units,[15−18] the transition temperatures associated with both crystalline melting and isotropization decrease with increasing the number of repeating units. This trend is believed to be attributed to an increase in the extent of packing constraints of rod segments as a result of more grafted coils per rod, and a decrease in the entropy caused by strong coil deformation occurred due to higher grafting density at the microphase-separated interface, as the number of repeating units increases.

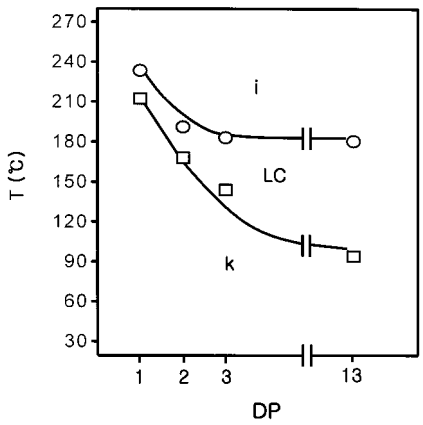

Figure 3. Dependence of the transition temperatures of the rod−coil multiblock oligomers and polymer on the degree of polymerization (DP). Data from the second heating scan: □, T_m; ○, T_{LC-i}.

X-ray Diffraction Studies. To investigate the supramolecular structures of the oligomers and polymer, X-ray scattering experiments were performed in their solid and melt states. The results of the small-angle diffraction measurements, the densities at 25 °C, and the number of rod−coil units that form a cross section of the columnar structures in the solid state are summarized in Table 2. Figure 4 presents the small-angle X-ray diffraction patterns of the oligomers and polymer measured in their solid state.

In the crystalline phases of $(rod-coil)_1$ **4**, the small-angle X-ray diffraction patterns display several sharp reflections which correspond to equidistant *q*-spacings and thus index to a lamellar lattice (Figure 4a). The layer spacing at the lower temperature crystalline phase of 90.4 Å is very close to the corresponding estimated molecular length, indicative of a monolayer lamellar structure in which rod segments are fully interdigitated. On heating to 154 °C, the layer spacing decreases to 82 Å, indicative of rod tilt with the angle of 28° relative to the layer normal. Further heating to 194 °C leads to a layer spacing of 78 Å, which indicates that the extent of the rod tilt increases with increasing temperature. This behavior can be explained by considering the coil segments to be conformationally flexible. On heating, higher thermal motion of flexible poly(propylene oxide) coils relative to that of rods leads to expansion of coils, consequently requiring more interfacial area. This spatial requirement results in the tilting transition which increases the average separation of grafting sites maintaining constant density in the rod domains. The tendency to result in tilting transition on heating or on increasing the coil volume fraction is consistent with the result described previously.[9] As shown in Figure 5a, the wide-angle diffraction patterns at the crystalline phases show sharp reflections at *q*-spacings of 13.2, 14.7, and 18.6 nm^{-1}, which are due to crystal packing of the rod segments within the aromatic domain. This result indicates that the rod segments pack in a rectangular lattice with unit cell dimensions of $a = 8.5$ Å and $b = 5.8$ Å.

In contrast to those of the crystalline phases, the small-angle X-ray diffraction pattern in the melt state shows several sharp reflections at the relative positions of $\sqrt{6}$, $\sqrt{8}$, $\sqrt{20}$, $\sqrt{22}$, $\sqrt{24}$, and $\sqrt{26}$ (Figure 6a). Similar to the results reported from our and other laboratories,[9a,b,12,19,20] these reflections can be indexed as a bicontinuous cubic phase with *Ia*3*d* symmetry with a

Table 2. Characterization by Small-Angle X-ray Scattering

		crystalline phase											liquid crystalline phase					
		lamellar			rectangular columnar					hexagonal columnar			cubic		tetragonal columnar		hexagonal columnar	
		k_1	k_2	k_3	lattice constant													
n	ρ_{25}[a] (g/mL)	d_{100} (Å)	d_{100} (Å)	d_{100} (Å)	d_{100} (Å)	d_{010} (Å)	a (Å)	b (Å)	n[b]	d_{100} (Å)	a (Å)	n[c]	d_{211} (Å)	a (Å)	d_{100} (Å)	a (Å)	d_{100} (Å)	a (Å)
1	1.11	90.4	81.6	78.3									69.8	170.5				
2	1.11				69.0	63.5	69.0	63.5	10.7						59.4	59.4		
3	1.11									56.2	64.9	9.0					53.6	61.9
13	1.11									50.4	58.2	7.3					50.2	57.9

[a] Experimental density at 25 °C. [b] Number of molecules per column cross section in rectangular columnar structure (n) = abh(N_A/M)ρ_{25}. [c] Number of molecules per column cross section in hexagonal columnar structure (n) = $(\sqrt{3}/2)a^2h(N_A/M)\rho_{25}$ [a, b = lattice constants, average inter-rod distance (h) = 4.78 Å, N_A = Avogadro's number, M = molecular weight of repeating unit].

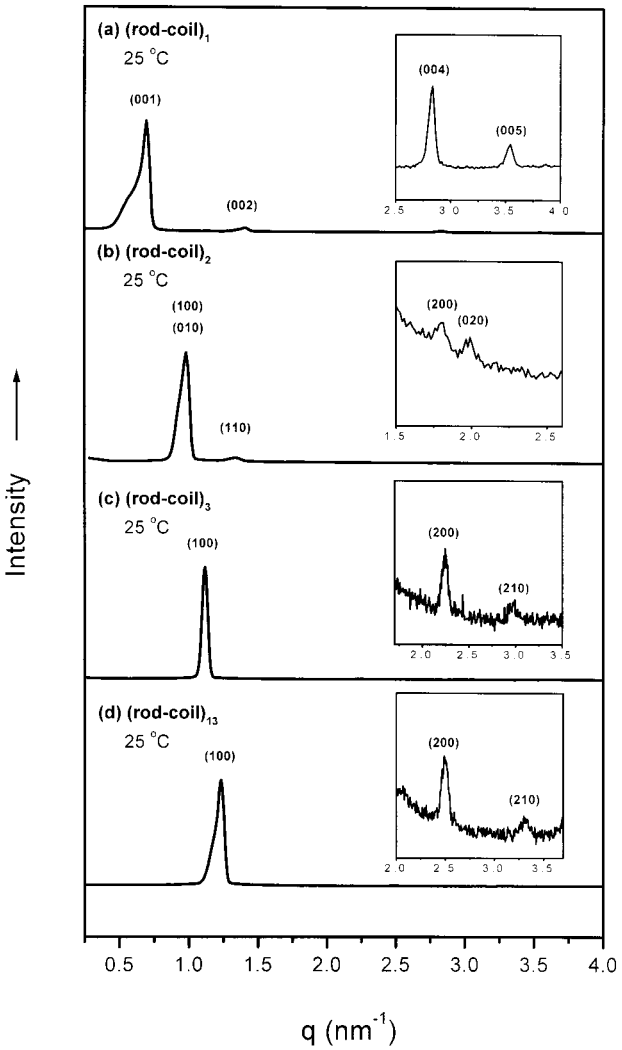

Figure 4. Small-angle X-ray diffraction patterns of the rod−coil multiblock oligomers and polymer measured in their solid state.

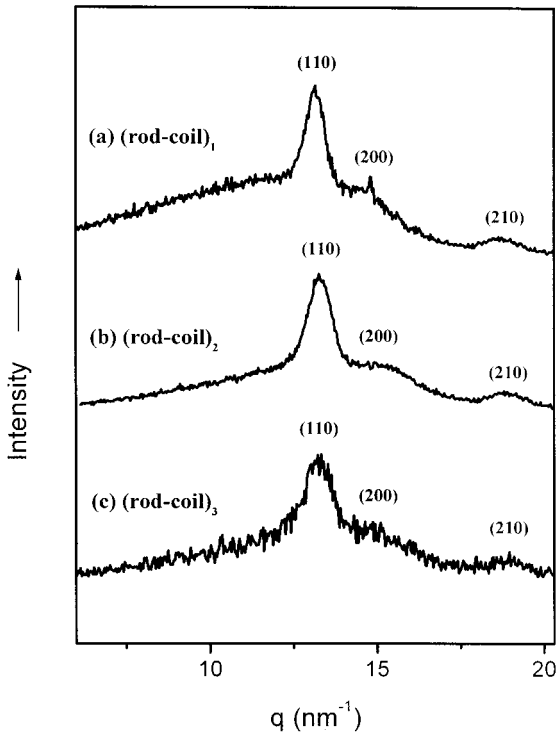

Figure 5. Wide-angle X-ray diffraction patterns of the rod−coil multiblock oligomers and polymer in their solid state.

lattice constant of 170.5 Å, while the WAXS pattern shows only a diffuse halo, corresponding to the disordered arrangement of the rod segments.

The small-angle X-ray diffraction pattern in the crystalline state of (rod−coil)$_2$ **6** shows strong overlapped reflections together with three sharp reflections of low intensity at the higher angles as shown in Figure 4b. The observed reflections can be indexed as (100), (010), (110), (200), and (020) planes of a 2-D rectangular symmetry with lattice parameters of a = 69.0 Å and b = 63.5 Å. Taking into account the lattice constants and measured density, the inner core of the rectangular column can be estimated to consist of striplike rod domains with a rectangular cross section with 51.1 Å in width and 30 Å in length as a result of parallel arrangement of 11 rod segments with their long axis (Table 2). While the wide-angle X-ray diffraction pattern shows two reflections at q-spacings of 13.2, 14.9, and 18.8 nm^{-1} (Figure 5b), which is similar diffraction pattern to that of the crystalline phase of the (rod−coil)$_1$. Therefore, the crystalline structure is considered to be essentially identical to that observed in the (rod−coil)$_1$.

In the melt state, the (rod−coil)$_2$ displays a strong small-angle X-ray reflection together with a weak reflection at higher angle, which can be indexed as (100) and (110) planes of a 2-D tetragonal lattice with a lattice constant of 59.4 Å (Figure 6b), while the WAXS pattern shows only a broad halo upon heating to the melt, indicative of the liquidlike correlations between the rod segments. These results together with optical polarized microscopic observations indicate that the (rod−coil)$_2$ exhibits an unusual tetragonal columnar liquid crystalline phase. Previously, the existence of a tetragonal columnar liquid crystalline structure has been observed

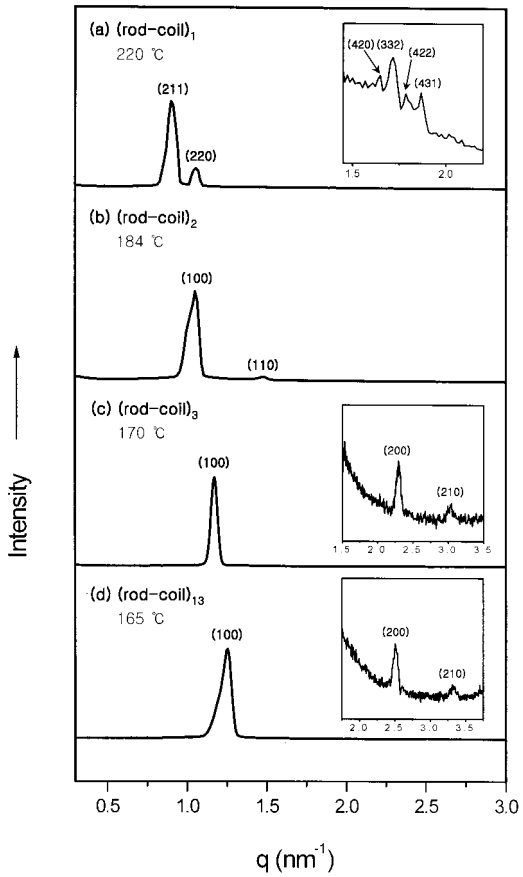

Figure 6. Small-angle X-ray diffraction patterns of the rod−coil multiblock oligomers and polymer measured in their melt state.

in disklike molecules such as bis(diphenylglyoximato)-Ni(II) complexes.[14]

The small-angle X-ray diffraction patterns for (rod−coil)$_3$ **8** and the polymer in their solid state display three sharp reflections with *d* spacings in the ratio of 1:$\sqrt{4}$:$\sqrt{7}$ (Figure 4c,d), characteristic of a 2-D hexagonal columnar structure. From the observed first-order reflections, the lattice constants can be estimated to be 65 and 58 Å for the (rod−coil)$_3$ and polymer, respectively. From the lattice constants and the measured densities, the average numbers of rod units per cross-sectional area of a cylinder can be calculated to be approximately 9 for the (rod−coil)$_3$ and 7 for the polymer (Table 2). As shown in Figure 5c, the wide-angle X-ray diffraction pattern of the (rod−coil)$_3$ at the crystalline state shows reflections, which are attributed to reflections from a rectangular lattice with lattice constants of $a = 8.4$ and $b = 5.7$ Å.

In the liquid crystalline phase of **8** and the polymer, the small-angle X-ray diffraction patterns display three reflections with an identical spacing ratio to that of the crystalline state, characteristics of the two-dimensional hexagonal structure (Figure 6c,d). The observed *d*-spacings and the lattice constants are summarized in Table 2. At wide angles only a diffuse halo remains as evidence of a lack of any positional long-range order within rod domains. Therefore, this liquid crystalline phase can be identified as a hexagonal columnar mesophase.

On the basis of the results described so far, the possible models responsible for the generation of the lamellar, 2-D rectangular, and 2-D hexagonal solid-state structures depending on the number of rod−coil repeating units can be presented as shown in Figure 7.

Discussion

The results described here represent that self-assembled solid-state structure, from 1-D lamellar, 2-D rectangular to 2-D hexagonal lattices, are formed by rod−coil structures that differ only in the number of repeating units. This variation of self-assembled structures, at an identical rod-to-coil volume ratio, can be rationalized by considering the density of grafting sites

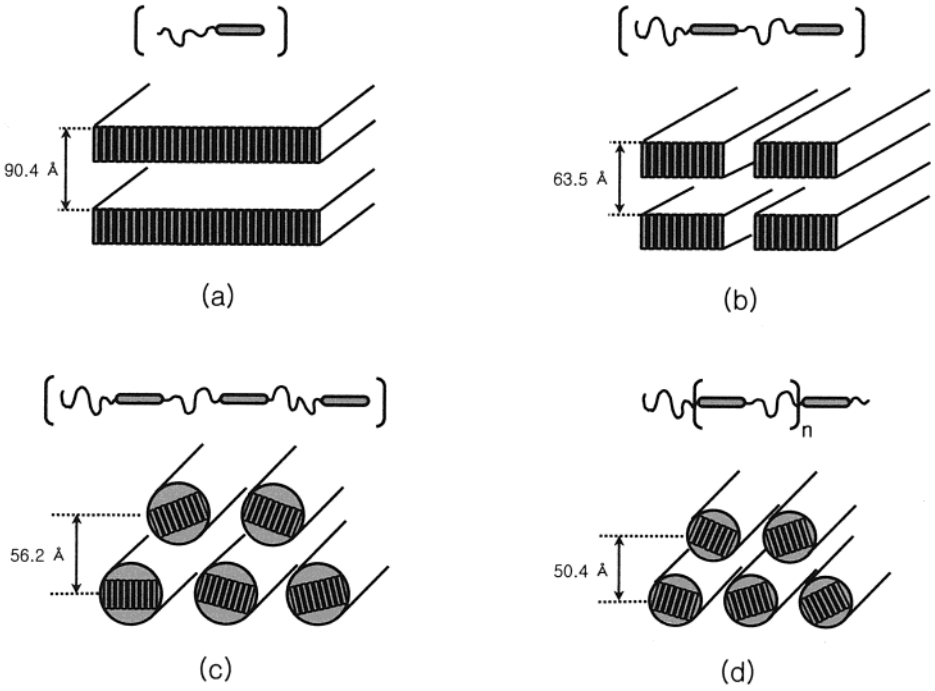

Figure 7. Schematic representation for the formation of (a) lamellar of the (rod−coil)$_1$, (b) 2-D rectangular of the (rod−coil)$_2$, (c) hexagonal columnar of the (rod−coil)$_3$, and (d) hexagonal columnar of the polymer.

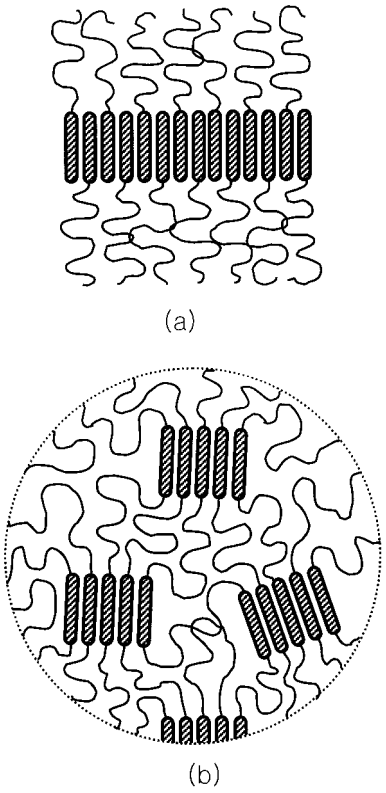

Figure 8. Schematic representation of the molecular arrangement of rod−coil units in (a) $(rod-coil)_1$ and (b) rod−coil multiblock copolymer. $(Rod-coil)_1$ consists of a rod grafted by a coil at only one end, giving rise to a lower grafting density at the interface, while rod−coil multiblock copolymer with infinite number of repeating units consists of rods grafted by coils at both ends, giving rise to a higher grafting density at the interface. The higher grafting density leads to coils to stretch away from the grafting site. To make room for coils to adopt a less stretched conformation, a sheetlike rod domain will break up into discrete domains.

at the interface separated by rod and coil segments as shown in Figure 8.[21,22] The $(rod-coil)_1$ with the coil grafted at only one end of the rod (the number of grafting sites per rod, $n_{graft} = 1$) gives rise to the formation of a fully interdigitated monolayer lamellar structure. This result indicates that the average separation of grafting sites in the monolayer lamellar structure is relatively large.

On increasing the number of repeating unit, the density of grafting sites at the interface will be increased due to an increase in the average number of coils grafted to a rod, which results in strong entropic penalty associated with coil stretching at the planar rod−coil interface. To reduce this coil stretching, the sheetlike rod domains will break up into 2-D discrete rectangular domains in which less confinement and deformation of coils occurs, thus lowering their free energy as in the case of the $(rod-coil)_2$ with $n_{graft} = 1.5$. On further increasing the number of repeating units, rod segments assemble into 2-D hexagonal domains with smaller lateral dimensions which allow more volume for coils to splay. Consequently, the $(rod-coil)_3$ ($n_{graft} = 1.67$) and the polymer ($n_{graft} = 1.92$) self-assemble into a hexagonal columnar structure. This splaying of the coils is reflected in the systematic reduction of the principal *d*-spacing with increasing the number of repeating units (Table 2), which implies that in-plane dimension of rod domains decreases as the number of repeating units increases (Figure 7).

The self-organization phenomena described for the series of rod−coil multiblock oligomers with an identical rod-to-coil volume ratio show that systematic variation in the average number of grafting sites per rod by means of increasing the number of repeating units can regulate the supramolecular architecture, from lamellar, rectangular columnar to hexagonal columnar lattices. The primary forces responsible for this structural change are believed to be the grafting density at the rod−coil interface and the resulting entropic penalty associated with coil stretching. This is in significant contrast to conventional self-organizing polymers such as coil−coil block copolymers[23,24] and liquid crystalline polymers based on rodlike building blocks[13b,16−18] in which the domain structure is essentially independent of the number of repeating units. Therefore, it is remarkable that the small variation in the number of repeating units of rod−coil multiblock oligomers results in a significant structural change in both their solid and melt states.

Conclusions

Linear rod−coil multiblock oligomers with an identical rod-to-coil volume fraction were synthesized and characterized, and their self-assembling behavior in the solid and melt states was investigated. These oligomers were observed to self-assemble into ordered structures that differ significantly as a function of the number of repeating units. The $(rod-coil)_1$ self-assembles into lamellar crystalline and bicontinuous cubic liquid crystalline structures. On the contrary, the $(rod-coil)_2$ exhibits a 2-D rectangular structure in the solid state and a tetragonal columnar structure in the melt state. Further increasing the number of repeating units gives rise to a hexagonal columnar structure in both the solid and melt states as in the case of the $(rod-coil)_3$ and the $(rod-coil)_{13}$. These results demonstrate that systematic variation of the number of repeating units, that is, the degree of polymerization in the rod−coil multiblock oligomers, can regulate the supramolecular structure, from lamellar, 2-D rectangular to 2-D hexagonal structures in the solid state and from 3-D bicontinuous cubic, tetragonal columnar to hexagonal columnar structures in the melt state. This is a significant contrast to conventional self-assembling polymers such as coil−coil block copolymers and liquid crystalline polymers based on rigid mesogenic units. This unique self-assembling behavior in the rod−coil multiblock oligomers with the same rod-to-coil volume fraction can be rationalized by considering the average number of grafting sites per rod and consequent grafting density at the interface separated by rod and coil segments.

Experimental Section

Materials. 4, 4′-Biphenol (99%), toluene-*p*-sulfonyl chloride (98%), 4-hydroxy-4′-methoxybiphenyl (99%), and 4,4′-bis(bromomethyl)biphenyl (99%) from Tokyo Kasei were used as received. Poly(propylene glycol)s ({DP} = 13) and tetrabutylammonium hydrogen sulfate (TBAH, 97%) from Aldrich and the other conventional reagents were used as received. 4-[Poly(propyleneoxy)propyloxy]-4′-bis(phenylphenol) (DP of poly(propylene oxide) (PPO) = 13) was synthesized according to the procedure described previously[12a] and then purified by silica gel column chromatography by using ethyl acetate as an eluent until polydispersity value remains constant at $\bar{M}_w/\bar{M}_n = 1.05$.

Techniques. ^{1}H NMR spectra were recorded from $CDCl_3$ solutions on a Bruker AM 250 spectrometer. The purity of the

products was checked by thin-layer chromatography (TLC; Merck, silica gel 60). A Perkin-Elmer DSC-7 differential scanning calorimeter equipped with 1020 thermal analysis controller was used to determine the thermal transitions, which were reported as the maxima and minima of their endothermic or exothermic peaks. In all cases, the heating and cooling rates were 10 °C min^{-1}. A Nikon Optiphot 2-pol optical polarized microscopy (magnification: 100×) equipped with a Mettler FP 82 hot stage and a Mettler FP 90 central processor was used to observe the thermal transitions and to analyze the anisotropic texture. Microanalyses were performed with a Perkin-Elmer 240 elemental analyzer at the Organic Chemistry Research Center. X-ray scattering measurements were performed in transmission mode with synchrotron radiation at the 3C2 X-ray beam line at Pohang Accelerator Laboratory, Korea. To investigate structural changes on heating, the sample was held in an aluminum sample holder which was sealed with the window of 7 μm thick Kapton films on both sides. The sample was heated with two cartridge heaters, and the temperature of the samples was monitored by a thermocouple placed close to the sample. The background scattering correction was made by subtracting the scattering from the Kapton. Molecular weight distributions ($\bar{M}_w/\bar{M}_n$) were determined by gel permeation chromatography (GPC) with a Waters R401 instrument equipped with a Styragel HR 3, 4, and 4E columns, a M7725i manual injector, a column heating chamber, and a 2010 Millennium data station. Measurements were made by using a UV detector and $CHCl_3$ as solvent (1.0 mL min^{-1}). The density (ρ) measurements of the molecules were performed in an aqueous sodium chloride solution at 25 °C.

Synthesis. The synthetic procedures used in the preparation of linear rod−coil multiblock oligomers and a polymer are described in Scheme 1.

Synthesis of 4-[Methyloxypoly(propyleneoxy)propyloxy]-4′-phenylphenol. 4-[Methyloxypoly(propyleneoxy)-propyloxy]-4′-phenylphenol was synthesized using a similar procedure described previously.[11]

2: Yield 70%. ^{1}H NMR (250 MHz, $CDCl_3$, δ, ppm): 7.38−7.44 (m, 4Ar−H, *m* to OH, *m* to OCH_2CH or $OCH(CH_3)$), 6.86−6.98 (m, 4Ar−H, *o* to OH, *o* to OCH_2CH or $OCH(CH_3)$), 4.53 (m, phenyl$OCH_2CH(CH_3)$ or $CH_2CH(CH_3)$Ophenyl), 3.20−3.85 (m, CH_3O and $OCH_2CH(CH_3)$), 0.85−1.40 (m, 39H, $CH(CH_3)O$). $\bar{M}_w/\bar{M}_n$ = 1.04 (GPC).

Synthesis of Compound 3. 2 (2.62 g, 2.58 mmol), 4,4′-bis(bromomethyl)biphenyl (7.40 g, 21.80 mmol), and excess K_2CO_3 were dissolved in 120 mL of acetone. The mixture was heated at reflux for 12 h and then cooled to room temperature. The solvent was removed in a rotary evaporator, and the resulting mixture was poured into water and extracted with methylene chloride. The methylene chloride solution was washed with water, dried over anhydrous magnesium sulfate, and filtered. After the solvent was removed in a rotary evaporator, the crude product was purified by column chromatography (silica gel) sequentially from methylene chloride and ethyl acetate eluents to yield 1.86 g (56%) of a white solid. ^{1}H NMR (250 MHz, $CDCl_3$, δ, ppm): 7.43−7.63 (m, 12Ar−H, *m* to OCH_2phenyl, *m* to OCH_2CH or $OCH(CH_3)$, *o* to CH_2-Ophenyl, *m* to CH_2Ophenyl, *o* to CH_2Br and *m* to CH_2Br), 6.96−7.06 (m, 4Ar−H, *o* to OCH_2phenyl, *o* to OCH_2CH or $OCH(CH_3)$), 5.14 (s, 2H, OCH_2phenyl), 4.53 (m, phenylOCH_2-$CH(CH_3)$ or $CH_2CH(CH_3)$Ophenyl, OCH_2Br), 3.18−3.82 (m, $OCH_2CH(CH_3)$ and OCH_3), 0.85−1.58 (m, 39H, $CH(CH_3)O$). $\bar{M}_w/\bar{M}_n$ = 1.04 (GPC).

Synthesis of (Rod−Coil)$_1$ 4. 3 (0.40 g, 0.31 mmol), 4-hydroxy-4′-methoxybiphenyl (0.33 g, 1.65 mmol), and excess K_2CO_3 were dissolved in 30 mL of acetone. The mixture was heated at reflux for 6 h and then cooled to room temperature. The solvent was removed in a rotary evaporator, and the resulting mixture was poured into water and extracted with methylene chloride. The methylene chloride solution was washed with water, dried over anhydrous magnesium sulfate, and filtered. After the solvent was removed in a rotary evaporator, the crude product was purified by column chromatography (silica gel) sequentially from methylene chloride−ethyl acetate (4:1) and ethyl acetate eluents to yield 0.38 g (86%) of a white solid. ^{1}H NMR (250 MHz, $CDCl_3$, δ, ppm): 7.44−7.65 (m, 16Ar−H, *m* to OCH_2phenyl, *m* to OCH_2CH or $OCH(CH_3)$, *m* to CH_3O, *o* to CH_2Ophenyl and *m* to CH_2-Ophenyl), 6.94−7.07 (m, 8Ar−H, *o* to OCH_2phenyl, *o* to OCH_2-CH or $OCH(CH_3)$ and *o* to CH_3O), 5.15 (s, 4H, OCH_2phenyl), 4.53 (m, phenyl$OCH_2CH(CH_3)$ or $CH_2CH(CH_3)$Ophenyl), 3.18−3.40 (m, $OCH_2CH(CH_3)$, phenylOCH_3 and OCH_3), 0.85−1.58 (m, 39H, $CH(CH_3)O$). $\bar{M}_w/\bar{M}_n$ = 1.04 (GPC). Anal. Calcd for $C_{79}H_{112}O_{17}$: C, 71.14; H, 8.46. Found: C, 71.13; H, 8.49.

Synthesis of Compound 5. 3 (1.12 g, 0.88 mmol), 4-[poly-(propyleneoxy)propyloxy]-4′-bis(phenylphenol) (DP of PPO = 13) (7.90 g, 7.13 mmol), and excess K_2CO_3 were dissolved in 250 mL of ethanol. The mixture was heated at reflux for 48 h and then cooled to room temperature. The solvent was removed in a rotary evaporator, and the resulting mixture was poured into water and extracted with methylene chloride. The methylene chloride solution was washed with water, dried over anhydrous magnesium sulfate, and filtered. After the solvent was removed in a rotary evaporator, excess 4-[poly(propyleneoxy)propyloxy]-4′-bis(phenylphenol) in the mixture was removed by column chromatography (silica gel, ethyl ether eluent). The resulting intermediate compound and excess 4,4′-bis(bromomethyl)biphenyl were dissolved in 50 mL of acetone, and excess K_2CO_3 was added. The mixture was heated at reflux for 6 h and then cooled to room temperature. The solvent was removed in a rotary evaporator, and the resulting mixture was poured into water and extracted with methylene chloride. The methylene chloride solution was washed with water, dried over anhydrous magnesium sulfate, and filtered. After the solvent was removed in a rotary evaporator, the crude product was purified by column chromatography (silica gel) sequentially from methylene chloride−ethyl acetate (4:1) and ethyl acetate eluents to yield 1.10 g (48%) of a white solid. ^{1}H NMR (250 MHz, $CDCl_3$, δ, ppm): 7.43−7.63 (m, 28Ar−H, *m* to OCH_2-phenyl, *m* to OCH_2CH or $OCH(CH_3)$, *o* to CH_2Ophenyl, *m* to CH_2Ophenyl, *o* to CH_2Br and *m* to CH_2Br), 6.96−7.06 (m, 12Ar−H, *o* to OCH_2phenyl, *o* to OCH_2CH or $OCH(CH_3)$), 5.14 (s, 6H, OCH_2phenyl), 4.53 (m, phenyl$OCH_2CH(CH_3)$ or $CH_2CH(CH_3)$Ophenyl, OCH_2Br), 3.18−3.90 (m, $OCH_2CH(CH_3)$ and OCH_3), 0.85−1.58 (m, 78H, $CH(CH_3)O$). $\bar{M}_w/\bar{M}_n$ = 1.06 (GPC).

Synthesis of (Rod−Coil)$_2$ 6. (Rod−coil)$_2$ **6** was obtained in 80% yield as a white solid using the similar procedure of the (rod−coil)$_1$, while the final purification of crude product was performed through column chromatography (silica gel) sequentially from methylene chloride−ethyl acetate (4:1) and methylene chloride−methanol (8:1) eluents. ^{1}H NMR (250 MHz, $CDCl_3$, δ, ppm): 7.44−7.65 (m, 32Ar−H, *m* to OCH_2-phenyl, *m* to OCH_2CH or $OCH(CH_3)$, *m* to CH_3O, *o* to CH_2-Ophenyl and *m* to CH_2Ophenyl), 6.94−7.07 (m, 16Ar−H, *o* to OCH_2phenyl, *o* to OCH_2CH or $OCH(CH_3)$ and *o* to CH_3O), 5.14 (s, 8H, OCH_2phenyl), 4.53 (m, phenyl$OCH_2CH(CH_3)$ or $CH_2CH(CH_3)$Ophenyl), 3.18−3.95 (m, $OCH_2CH(CH_3)$, phenyl-OCH_3 and OCH_3), 0.85−1.58 (m, 78H, $CH(CH_3)O$). $\bar{M}_w/\bar{M}_n$ = 1.05 (GPC). Anal. Calcd for $C_{156}H_{218}O_{33}$: C, 71.47; H, 8.38. Found: C, 71.48; H, 8.48.

Synthesis of Compound 7. 7 was synthesized using the same procedure of **5** and obtained in 41% yield as a white solid. ^{1}H NMR (250 MHz, $CDCl_3$, δ, ppm): 7.43−7.63 (m, 44Ar−H, *m* to OCH_2phenyl, *m* to OCH_2CH or $OCH(CH_3)$, *o* to CH_2-Ophenyl, *m* to CH_2Ophenyl, *o* to CH_2Br and *m* to CH_2Br), 6.96−7.06 (m, 20Ar−H, *o* to OCH_2phenyl, *o* to OCH_2CH or $OCH(CH_3)$), 5.14 (s, 10H, OCH_2phenyl), 4.53 (m, phenylOCH_2-$CH(CH_3)$ or $CH_2CH(CH_3)$Ophenyl, OCH_2Br), 3.18−3.92 (m, $OCH_2CH(CH_3)$ and OCH_3), 0.85−1.58 (m, 117H, $CH(CH_3)O$). $\bar{M}_w/\bar{M}_n$ = 1.08 (GPC).

Synthesis of (Rod−Coil)$_3$ 8. (Rod−coil)$_3$ **8** was synthesized using the same procedure of the (rod−coil)$_2$ and obtained in 82% yield as a white solid. ^{1}H NMR (250 MHz, $CDCl_3$, δ, ppm): 7.44−7.65 (m, 48Ar−H, *m* to OCH_2phenyl, *m* to OCH_2CH or $OCH(CH_3)$, *m* to CH_3O, *o* to CH_2Ophenyl and *m* to CH_2-Ophenyl), 6.94−7.07 (m, 24Ar−H, *o* to OCH_2phenyl, *o* to OCH_2-CH or $OCH(CH_3)$ and *o* to CH_3O), 5.14 (s, 12H, OCH_2phenyl), 4.53 (m, phenyl$OCH_2CH(CH_3)$ or $CH_2CH(CH_3)$Ophenyl), 3.18−3.95 (m, $OCH_2CH(CH_3)$, phenylOCH_3 and OCH_3), 0.85−1.58

(m, 117H, CH(CH_3)O). $\bar{M}_w/\bar{M}_n$ = 1.08 (GPC). Anal. Calcd for $C_{233}H_{324}O_{49}$: C, 71.59; H, 8.35. Found: C, 71.59; H, 8.34.

Synthesis of Rod−Coil Multiblock Copolymer. Polymer was obtained in 70% yield using the same procedure described previously.[12a] ^{1}H NMR (250 MHz, $CDCl_3$, δ, ppm): 7.43−7.65 (m, 16Ar−H, *m* to OCH_2phenyl, *m* to OCH_2CH, *m* to OCH(CH_3), *o* to CH_2Ophenyl and *m* to CH_2Ophenyl), 6.95−7.06 (m, 8Ar−H, *o* to OCH_2phenyl, *o* to OCH_2CH and *o* to $OCH(CH_3)$), 5.13 (s, 4H, OCH_2phenyl), 4.53 (m, 3H, phenyl$OCH_2CH(CH_3)$ and $CH_2CH(CH_3)$Ophenyl), 3.20−3.85 (m, 39H, $OCH_2CH(CH_3)$), 0.85−1.45 (m, 39H, CH(CH_3)O). $\bar{M}_n$ = 16 700 (GPC); $\bar{M}_w/\bar{M}_n$ = 1.29 (GPC). Anal. Calcd for $C_{77}H_{106}O_{16}$: C, 71.82; H, 8.29. Found: C, 71.84; H, 8.28.

Acknowledgment. Financial support of this work by CRM-KOSEF (2000) and Pohang Accelerator Laboratory, Korea (for the beam time and technical assistance), is gratefully acknowledged. B.-K.C acknowledges the BK 21 fellowship from the Ministry of Education, Korea. W.-C.Z is grateful to the POSTECH research fund.

References and Notes

(1) Muthukumar, M.; Ober, C. K.; Thomas, E. L. *Science* **1997**, *277*, 1225.
(2) Martinez, J. S.; Zhang, G. P.; Holt, P. D.; Jung, H.-T.; Carrno, C. J.; Haygood, M. G.; Butler, A. *Science* **2000**, *287*, 1245.
(3) De Rosa, C.; Park, C.; Thomas, E. L.; Lotz, B. *Nature* **2000**, *405*, 433.
(4) Foester, S.; Antonietti, M. *Adv. Mater.* **1998**, *10*, 195.
(5) Percec, V.; Ahn, C. H.; Ungar, G.; Yeardley, D. J. P.; Möller, M.; Sheiko, S. S. *Nature* **1998**, *391*, 161.
(6) (a) Sakamoto, N.; Hashimoto, T. *Macromolecules* **1998**, *31*, 8493. (b) Stadler, R.; Auschra, C.; Beckmann, J.; Kappe, U.; Voigt-Martin, I.; Leibler, L. *Macromolecules* **1995**, *28*, 3080. (c) Stocker, W.; Beckmann, J.; Stadler, R.; Rabe, J. P. *Macromolecules* **1996**, *29*, 7502.
(7) (a) Stupp, S. I.; LeBonheur, V.; Walker, K.; Li, L. S.; Huggins, K. E.; Kesser, M.; Amstutz, A. *Science* **1997**, *276*, 384. (b) Radzilowski, L. H.; Carragher, B. O.; Stupp, S. I. *Macromolecules* **1997**, *30*, 2110.
(8) (a) Jenecke, S. A.; Chen, X. L. *Science* **1998**, *279*, 1903. (b) Jenecke, S. A.; Chen, X. L. *Science* **1999**, *283*, 372.
(9) (a) Lee, M.; Cho, B.-K.; Kim, H.; Yoon, J.-Y.; Zin, W.-C. *J. Am. Chem. Soc.* **1998**, *120*, 9168. (b) Lee, M.; Cho, B.-K.; Kim, H.; Zin, W.-C. *Angew. Chem., Int. Ed. Engl.* **1998**, *37*, 638. (c) Lee, M.; Cho, B.-K. *Chem. Mater.* **1998**, *10*, 1849. (d) Lee, M.; Oh, N.-K.; Zin, W.-C. *Chem. Commun.* **1996**, 1787. (e) Cho, B.-K.; Ryu, J.-H.; Zin, W.-C.; Lee, M. *Polym. Bull.* **2000**, *44*, 393.
(10) Lee, M.; Lee, D.-W.; Cho, B.-K.; Yoon, J.-Y.; Zin, W.-C. *J. Am. Chem. Soc.* **1998**, *120*, 13258.
(11) Lee, M.; Cho, B.-K.; Jang, Y.-G.; Zin, W.-C. *J. Am. Chem. Soc.* **2000**, *122*, 7449.
(12) (a) Lee, M.; Cho, B.-K.; Kang, Y.-S.; Zin, W.-C. *Macromolecules* **1999**, *32*, 7688. (b) Lee, M.; Cho, B.-K.; Kang, Y.-S.; Zin, W.-C. *Macromolecules* **1999**, *32*, 8531.
(13) (a) Zhang, J.; Moore, J. S.; Xu, Z.; Agguire, A. A. *J. Am. Chem. Soc.* **1992**, *114*, 2273. (b) Percec, V.; Asandei, A. D. *Macromolecules* **1997**, *30*, 7701.
(14) Ohta, K.; Higashi, R.; Ikejima, M.; Yamamoto, I.; Kobayashi, N. *J. Mater. Chem.* **1998**, *8*, 1979.
(15) Prest, P.-J.; Prince, R. B.; Moore, J. S. *J. Am. Chem. Soc.* **1999**, *121*, 5933.
(16) Percec, V.; Kawasumi, M. *Macromolecules* **1993**, *26*, 3663.
(17) Percec, V.; Lee, M. *Macromolecules* **1991**, *24*, 2780.
(18) Laus, M.; Angeloni, A. S.; Spagna, A.; Galli, G.; Chiellini, E. *J. Mater. Chem.* **1994**, *4*, 437.
(19) Lee, M.; Cho, B.-K.; Yoon, J.-Y.; Zin, W.-C. *Mol. Cryst. Liq. Cryst.* **1999**, *332*, 83.
(20) Tsiourvas, D.; Kardassi, D.; Paleos, C. M.; Gehant, S.; Skoulios, A. *Liq. Cryst.* **1997**, *23*, 269.
(21) Halperin, A. *Macromolecules* **1990**, *23*, 2724.
(22) (a) Williams, D. R. M.; Fredrickson, G. H. *Macromolecules* **1992**, *25*, 3561. (b) Semenov, A. N.; Vasilenko, S. V. *Sov. Phys. JETP* **1986**, *63*, 70. (c) Semenov, A. N.; Subbotin, A. N. *Sov. Phys. JETP* **1992**, *74*, 660. (d) Müller, M.; Schick, M. *Macromolecules* **1996**, *29*, 8900. (e) Matsen, M. W.; Barrett, C. *J. Chem. Phys.* **1998**, *109*, 4108. (f) Halperin, A. *Europhys. Lett.* **1989**, *10*, 549. (g) Raphael, E.; de Genn, P. G. *Makromol. Chem., Macromol. Symp.* **1992**, *62*, 1. (h) Sevick, E. M.; Williams, D. R. M. *Colloids Surf.* **1997**, *387*, 129.
(23) Zielinski, J. M.; Spontak, R. J. *Macromolecules* **1992**, *25*, 653.
(24) Matsushita, Y.; Mogi, Y.; Mukai, H.; Watanabe, J.; Noda, I. *Polymer* **1994**, *35*, 246.

MA001938F